however, develops at a faster rate and the stratification in the vapour zone is clearly defined (Fig. 7.b).

6. CONCLUDING REMARKS

The characteristics of the transient free convection in a partially filled horizontal cylinder with Dirichlet and Newmann thermal boundary conditions have been studied numerically.

The coordinate transformation technique combined with segregated technique for solving the Boussinesq correction equations is described and it is demonstrated how the inherent geometric difficulties of the domain of interest are overcome.

The overall algorithm have been tested using analytical and experimental data available in the literature and satisfactory agreement is observed.

Acknowledgment

This work has been financially supported by Transportation Development Centre (Transport Canada) and Natural Sciences and Engineering Research Council of Canada.

References:

1. OSTRACH, S. - 'A Boundary Layer Problem in the Theory of Free Convection', Ph.D. Thesis, Brown University, 1950.
2. MARTINI, W.R. and CHURCHILL, S.W. - 'Natural Convection Inside a Horizontal Cylinder', A.I.Ch.E.J., 1960, 6, 251.
3. HELLUMS, J.D. and CHURCHILL, S.W. - 'Transient and Steady State Free and Natural Convection, Numerical Solutions: part 1, A.I.Ch.E.J. 8, 1962, 690.
4. BROOKS, I. and OSTRACH, S. - 'An Experimental Investigation of Natural Convection in a Horizontal Cylinder', J. Fluid Mechanics, 44, 1970, 545.
5. AYDEMIR, N.U. SOUSA, A.C.M. and VENART, J.E.S., -'Transient Thermal Stratification in Heated Partially Filled Horizontal Cylindrical Tanks', the 22nd ASME/AIChE National Heat Transfer Conference, ASME Paper No. 84-HT-60, 1984.
6. AYDEMIR, N.U., SOUSA, A.C.M. and VENART, J.E.S., - 'Transient Laminar Free Convection in Horizontal Cylinders', Warme and Stoffubertragung, 20, 1986, 59.
7. GRAY, D.D. and GIORGINI, A. - 'The Validity of the Boussinesq Approximation for Liquids and Gases', Int. J. Heat Mass Transfer, 19, 1976, 545.
8. VAN-DOORMAAL, J.P. and RAITHBY, G. - 'Enhancements of the SIMPLE Method for Predicting Incompressible Fluid Flows', Numerical Heat Transfer, 7, 1984, 147.
9. ARPACI, V.S. - Conduction Heat Transfer, Addison-Welsey, Massachusetts, 1966.

LOCAL EFFECTS OF HIGHLY NONORTHOGONAL GRIDS IN THE SOLUTION OF HEAT TRANSFER PROBLEMS IN CUSPED CORNERS

C.R.MALISKA AND A.F.C SILVA
MECHANICAL ENGINEERING DEPARTMENT
FEDERAL UNIVERSITY OF SANTA CATARINA
P.O.BOX 476 -FLORIANOPOLIS -SC - BRAZIL

ABSTRACT

A boundary fitted coordinate method is applied to the solution of the fully developed laminar flow in a cusped corner with the main goal of investigating the local effects of the grid nonorthogonality. Because nonorthogonal grids originate transformed equations which involve cross derivatives in the diffusion terms, there have been considerable effort in developing methods to generate orthogonal grids to be used in conjunction with orthogonal schemes. This also tries to avoid the alleged complexity of the nonorthogonal models.

In this work several questions related to the use of nonorthogonal models are addressed. Among them are the analysis of the effect of the grid nonorthogonality upon the accuracy of the results, as well as a discussion about the generality of boundary fitted orthogonal and nonorthogonal models.

NOMENCLATURE

x,y,z - Cartesian Coordinate System
ξ,η,Γ - General Coordinate System
ω - Axial Velocity
T - Temperature
ρ - Density
μ - Viscosity
c_p - Specific Heat
dP/dz - Pressure Gradient in the Axial Direction
k - Thermal Conductivity
J - Jacobian of the Transformation
α,β,γ - Components of the Metric Tensor
C_1, C_1^* - $\mu J\alpha$, $kJ\alpha/c_p$
C_2, C_2^* - $\mu J\beta$, $-kJ\beta/c_p$
C_4, C_4^* - $\mu J\gamma$, $kJ\gamma/c_p$

$\overline{T}_s, T_b$ - Surface and Bulk Temperature
$\overline{Nu}$ - Average Nusselt Number

1. INTRODUCTION

The use of boundary fitted coordinates has become an efficient tool for the solution of heat transfer and fluid flow problems. Problems defined in irregular geometries that would involve complex and cumbersome computer codes, if cartesian discretization were adopted, can today be formulated and solved in a elegant framework. Thus, the use of boundary fitted coordinates, in conjunction with finite volume techniques, is now appearing as the most promising route to obtain general and powerfull computer codes.

Concerning to the type of coordinate system a relevant question is still open to the numerical analyst. What type of numerical model to develop, an orthogonal or a nonorthogonal one ? For the orthogonal models it is claimed the advantage in not having cross derivative terms to be modelled, avoiding then the nine points stencil. Such a method is, however, restricted to the use of orthogonal discretizations. Nonorthogonal models, in the other hand, taking proper care of the cross derivative terms, can manage any type of discretization like orthogonal, quasi-orthogonal and nonorthogonal. This ability of the model is a very important and desired feature to be pursued if one wants to take full advantage of the highly sophisticated computer technology available nowadays.

For example, if a grid is to be constructed in a very complex domain with sharp corners it may be very difficult to obtain an orthogonal, or even a nonorthogonal, grid with some specified grid resolution, using an automatic grid generator. It may be necessary to adjust the grid interacting with a graphic terminal resorting on the best grid generator method: the human eye associated with insight into the physics of the phenomenon to be studied. Of course, the grid adjusted in this way can only be used if a nonorthogonal model is available.

In this paper attention is foccused on the influence of the grid nonorthogonality upon the numerical results. Not too much effort has been devoted to investigate these influences |1| compared with the effort in developing and applying nonorthogonal models for heat transfer problems. To accomplish this task a model described in |2| is applied to solve the fully developed laminar flow in a 4-cusp duct. Two different discretizations are adopted; a highly nonorthogonal and a quasi-orthogonal one. The results obtained are complemented with the ones obtained by solving a heat conduction problem in an annulus using orthogonal and nonorthogonal grids.

2. PROBLEM STATEMENT

The problem under consideration is the fully developed laminar incompressible flow of a Newtonian fluid in a 4-cusp duct as shown in Fig. 1. This problem is of interest in the

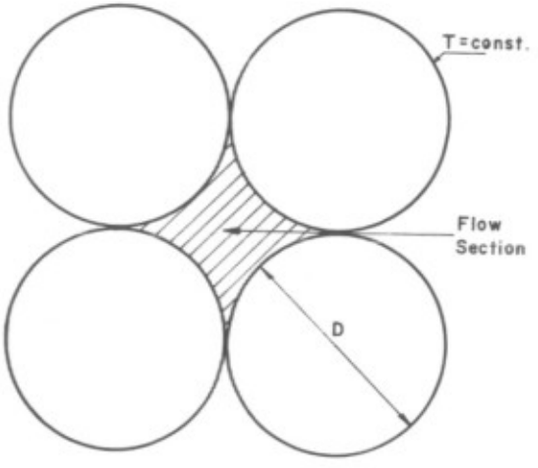

Fig.1 - Geometry under Consideration

nuclear reactor technology in the prediction of the critical cooling conditions in case of an accident. Experimental results for the laminar case for this type of duct are reported in |4|. Unfornately no useful informations to be used in this paper can be extracted from |4|. The analysis of the turbulent flow in a 3-cusp duct using a finite volume method with orthogonal discretization is reported in |3|.

Written in the Cartesian coordinate system the momentum equation in the axial direction and the energy equation are

$$\frac{dP}{dz} = \frac{\partial}{\partial x}\left(\mu\frac{\partial w}{\partial x}\right) + \frac{\partial}{\partial y}\left(\mu\frac{\partial w}{\partial y}\right) \qquad (1)$$

$$\frac{\partial}{\partial z}(\rho w T) = \frac{\partial}{\partial x}\left(\frac{k}{c_p}\frac{\partial T}{\partial x}\right) + \frac{\partial}{\partial y}\left(\frac{k}{c_p}\frac{\partial T}{\partial y}\right) \qquad (2)$$

the boundary conditions can be inferred from Fig.1. The above equations written in the ξ, η, Γ coordinate system take the following form

$$\frac{1}{J}\frac{dP}{d\Gamma} = \frac{\partial}{\partial\xi}\left(C_1\frac{\partial w}{\partial\xi}\right) + \frac{\partial}{\partial\eta}\left(C_4\frac{\partial w}{\partial\eta}\right) + \underline{\frac{\partial}{\partial\xi}\left(C_2\frac{\partial w}{\partial\eta}\right) + \frac{\partial}{\partial\eta}\left(C_2\frac{\partial w}{\partial\xi}\right)} \qquad (3)$$

$$\frac{\partial}{\partial\Gamma}(\rho w T) = \frac{\partial}{\partial\xi}\left(C_1^*\frac{\partial T}{\partial\xi}\right) + \frac{\partial}{\partial\eta}\left(C_4^*\frac{\partial T}{\partial\eta}\right) + \underline{\frac{\partial}{\partial\xi}\left(C_2^*\frac{\partial T}{\partial\eta}\right) + \frac{\partial}{\partial\eta}\left(C_2^*\frac{\partial T}{\partial\xi}\right)} \qquad (4)$$

where

$$W = \frac{w}{J} \tag{5}$$

The terms underlined in Eqs.(3) and (4) are the nonorthogonal ones since they involve the metric tensor component β which is zero for an orthogonal transformation. The problem defined by Eqs.(3) and (4) with the appropriate boundary conditions is solved using the finite-volume method described in |2|. The problem is solved using the dicretizations shown in Fig.2.

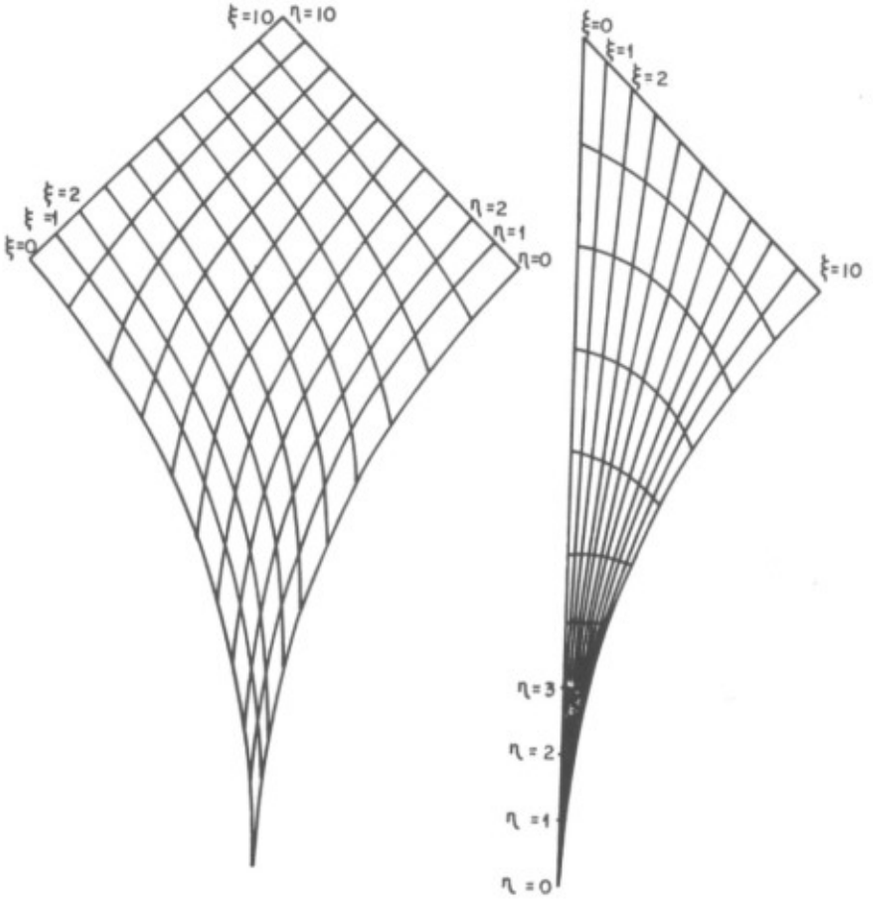

Fig.2 -Domain Discretizations

Both grids were obtained by solving a suitable elliptic system of equations |5|.

Before to present the numerical results it is appropriate to define a way to measure the nonorthogonality of the grid. This is done in the next section.

3. GRID NONORTHOGONALITY DEGREE (GND)

In analysing local effects of the grid nonorthogonality it is necessary to have a clear measure of this condition. The existence of a β factor different from zero, of course, characterizes that the grid is nonorthogonal. However, the magnitude of β can not be used as a measure of the degree of nonorthogonality because it depends on the absolute values of the coordinate points in the physical and transformed domains. It is necessary then to normalize the β value. This is equivalent as to define the cossine of the angle between grid lines. Evaluating this angle in every point of the domain one has a picture of the local nonorthogonality of the grid.

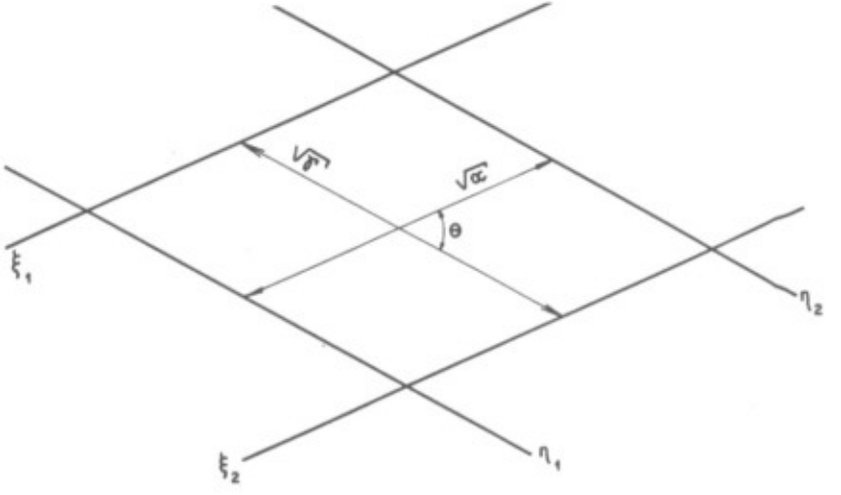

Fig.3 - Definition of the GND

To evaluate the angle θ, as shown in Fig.3, the dot product between the base vectors along the ξ and η coordinates is taken. Following tensor relations one gets

$$\cos\theta = \frac{\beta}{\sqrt{\alpha}\,\sqrt{\gamma}} \equiv \mathrm{GND} \tag{6}$$

where α, β and γ are define as

$$\alpha = x_\eta^2 + y_\eta^2 \tag{7}$$

$$\beta = x_\xi x_\eta + y_\xi y_\eta \tag{8}$$

$$\gamma = x_\xi^2 + y_\xi^2 \tag{9}$$

The parameter GND varies from +1 to -1 while its

corresponding angle varies from 0 to 180 . For an orthogonal grid GND is equal to zero.

4. Numerical Results of the Heat Transfer Problem.

The heat transfer problem defined by Eqs.(3) and (4) was solved using the discretization shown in Fig.2. As can be seen the "non-polar" grid is highly nonorthogonal near the cusped corner while the "polar grid is quasi-orthogonal in this region. Table 2 shows the GND factor for the "non-polar grid". In the same table it is shown the GND values along the ξ=0 coordinate line. As can be seen the GND reaches values close to 1, which means that the ξ and η lines are almost parallel in these locations. A 10x10 mesh was employed for both grids and no grid resolution study was carried out since there is no interest in reporting in this paper the exact nusselt number for the problem. The main goal, as already pointed out, is to identify possible sources of inaccuracies due to the use of excessively distorted meshes, as is the case of the "non-polar"grid.

Fig.4 shows the local Nusselt number along the wall for both discretizations and Table 1 shows the numerical values, being line (a) for the quasi-orthogonal grid and line (b) for the highly nonorthogonal one. The angle α^* defines the position where the Nusselt number is calculated.

Table 1 - Local Nusselt Number

α^*	2.25	6.75	11.25	15.75	20.25	24.75	29.25	33.75	38.25	42.75
a	0.00	0.00	0.01	0.13	0.73	1.98	4.60	8.20	11.33	12.79
b	0.36	-0.11	-0.41	-0.27	0.60	2.39	5.08	8.25	11.15	12.86

The first important conclusion to be draw from this figure is the fact that for engineering calculations both grids are suitable, since the useful parameter, the average Nusselt number, differ from each other by about 0.3%. The agreement of the local Nusselt number is also good for the entire wall.

Attention should be foccused, however, on the region close to the cusped corner. In this region the "polar" grid is almost orthogonal with the GND values close to zero while the "non polar" grid exhibit GND values close to 1 as can be seen in Table 2. The local Nusselt number for the "non-polar" grid shows negative values near the corner, i.e. for α^* from 0 to 18, while for the quasi-orthogonal grid the Nusselt number decreases smoothly to zero in this region. The negative values obtained near the corner are of the order of only 3% of the maximum value, and this is the reason why the average Nusselt number is in excellent agreement for both grids. In the numerical point of view, however, these are findings that deserve deeper investigation.

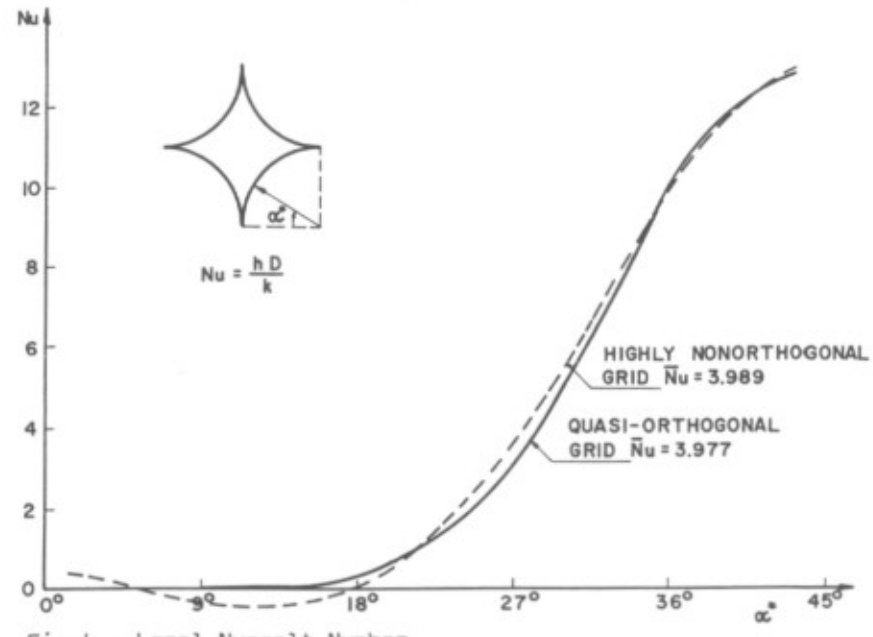

Fig.4 - Local Nusselt Number

Table 2 - GND for the"non-polar" grid

ξ \ η	0-1	1-2	2-3	3-4	4-5	5-6	6-7	7-8	8-9	9-10
0 - 1	.997	.987	.971	.946	.910	.857	.776	.650	.454	.179
1 - 2	.987	.971	.945	.908	.855	.780	.678	.542	.369	.175
2 - 3	.971	.945	.907	.853	.781	.691	.581	.453	.311	.170
3 - 4	.946	.908	.853	.782	.695	.598	.493	.382	.268	.162
4 - 5	.910	.855	.781	.695	.603	.509	.415	.322	.232	.149
5 - 6	.857	.780	.691	.598	.509	.425	.345	.269	.197	.131
6 - 7	.776	.678	.581	.493	.415	.345	.281	.220	.162	.110
7 - 8	.650	.542	.453	.382	.322	.269	.220	.172	.127	.084
8 - 9	.454	.369	.311	.268	.232	.197	.162	.127	.091	.057
9 -10	.179	.175	.170	.162	.149	.131	.110	.084	.057	.028
0	.999	.993	.980	.960	.930	.885	.814	.696	.495	.179

It is evident, inspecting Fig. 2, that the "non polar" grid is highly nonorthogonal near the corner, but it is also important to note that the grid size changes significantly in the same region. To investigate these effects, namely the grid nonorthogonality and the grid nonuniformity, a heat conduction problem in an annulus, with uniform heat generation and prescribed constant temperature at the surfaces, is solved.

5. Investigation on the Effect of the Grid Shape

Consider the problem of solving the heat conduction equation in an annulus. The governing equation is

$$\frac{\partial}{\partial x}(k\frac{\partial T}{\partial x}) + \frac{\partial}{\partial y}(k\frac{\partial T}{\partial y}) + \dot{q} = 0 \qquad (10)$$

with T=0 at the surfaces. It is important to point out that this problem if written in polar coordinates is onedimensional, but in Cartesian coordinates it is two-dimensional. Eq.(10) transformed to the ξ - η domain takes the form

$$-\frac{\dot{q}}{Jc_p} = \frac{\partial}{\partial \xi}(C_1^*\frac{\partial T}{\partial \xi}) + \frac{\partial}{\partial \eta}(C_4^*\frac{\partial T}{\partial \eta}) + \frac{\partial}{\partial \xi}(C_2^*\frac{\partial T}{\partial \eta}) + \frac{\partial}{\partial \eta}(C_2^*\frac{\partial T}{\partial \xi}) \qquad (11)$$

Since the boundary conditions are symmetric with respect to the angular direction ϕ the solution of this problem must give a temperature field whose isotherms are concentric circles. The solution of Eq.(11), using the grids shown in Fig. 5, will permit to draw important conclusions with respect to the grid nonorthogonality and to the grid spacing.

A 10x36 grid was used for the uniformly spaced grids and a 10x40 for the nonunformly spaced ones, with the configuration shown in Fig.5. The η lines are not shown in the figure but in all cases they are concentric circles.

Problem (a) - Orthogonal Grid - Uniformly Spaced

In this case the GND for every point in the domain is equal to zero. The local heat flux at the inner boundary divided by the average heat flux is shown in Table 3. The solution obtained clearly shows that the temperature field is independent of ϕ, as expected.

Problem (b) - Orthogonal Grid - Nonuniformly Spaced

For this situation the grid is shown in Fig.5(b). The results for this case are shown in Table 3 (line b) where it can be seen that the local heat flux is not constant with ϕ showing a maximum deviation of 17%. These results are somewhat surprising since the grid is apparently orthogonal. A deeper look, however, will reveal that the grid is not orthogonal in every point.

To illustrate this consider the two nonuniform cells denoted by P and E in Fig.6. To evaluate the GND at the point P the angle θ involved will be formed by the intersection of

the line joining points w and e with the radial line passing through P.

This, of course, will result in a GND equal to zero (orthogonal). The same holds for the GND value at the point E and for the central point of every cell in the domain.

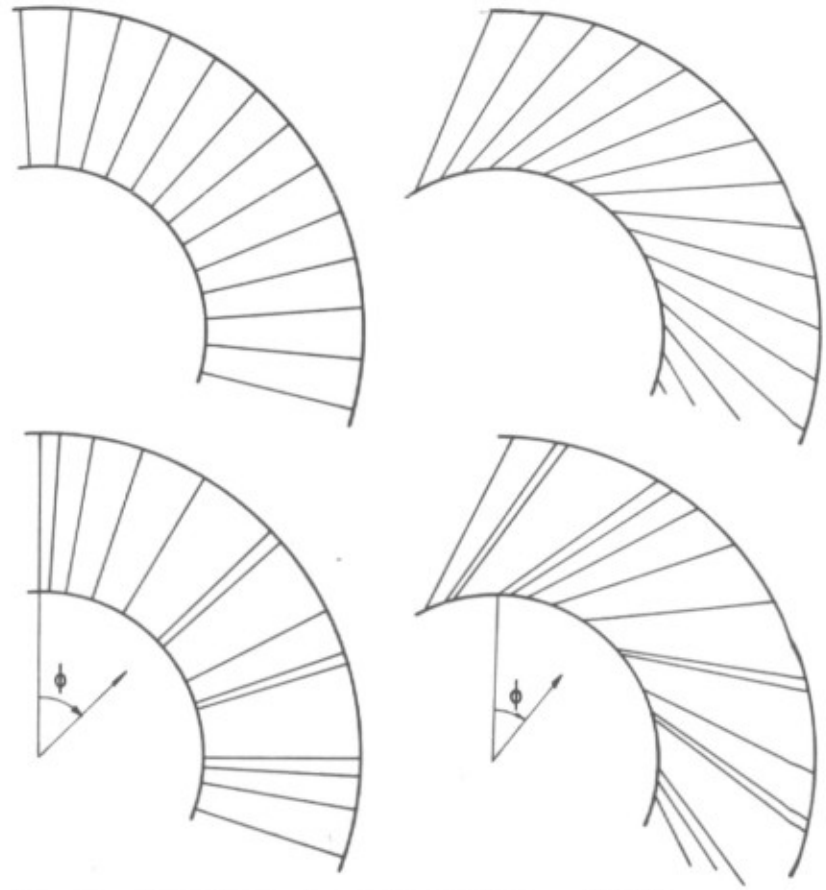

Fig. 5 - Nonorthogonal and Quasi-Orthogonal Grids

Table 3 - Local Heat Flux Distribution

ϕ	1.5	6.0	13.5	24.0	32.5	46.5	55.5	66.0	70.0	80.5
a	1.000	1.000	1.000	1.000	1.000	1.000	1.000	1.000	1.000	1.000
b	1.132	1.044	1.011	1.000	0.973	1.170	0.964	1.078	1.176	0.939
c	0.995	0.998	1.000	1.001	1.001	0.995	1.001	0.996	0.993	1.002
d	1.000	1.000	1.000	1.000	1.000	1.000	1.000	1.000	1.000	1.000
e	1.191	1.098	1.041	1.008	0.934	1.292	0.939	1.138	1.366	0.886
f	1.114	1.051	1.019	1.004	0.965	1.173	0.964	1.080	1.210	0.935

The calculation of GND at the interfaces of the control

volumes shows different results. Reporting again to Fig.6 the angle θ at the point e is formed by intersection of the lines joining point E and P with the radial line passing through the point e. It is clear that the GND will not be zero.It will only when Pe equals Ee, reducing then to the case of uniformly spaced grids.

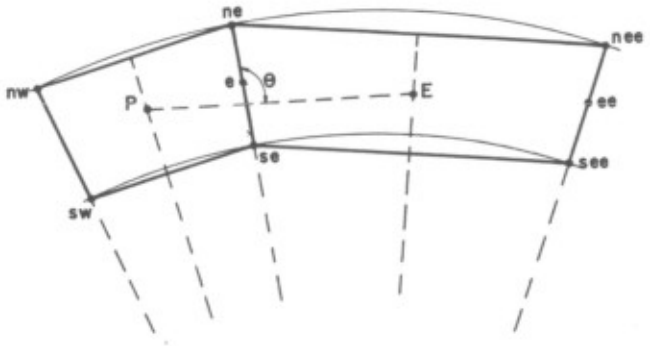

Fig. 6 - Calculation of β at Interfaces

What must be stressed here is that this nonorthogonality is due to the way that the metric β is calculated, which assumes straight lines joining coordinate points. If the grid is uniformly spaced the straight lines suffice, but if it is not, assuming a straight line joining points P and E introduces an artificial or numerical nonorthogonality. This suggests that this procedure for calculating the β metric at the interfaces of the control volumes needs to be revised.

Problem (c) - Orthogonal Grid - Nonuniformly Spaced - β Calculated in a Different Manner

Since in the previous problem the values of β at the center of the cells were correctly calculated it is reasonable to calculate the metric at the interface as an average of the central ones. Doing this the metric will be zero at every point (centre and interfaces).Table 3 (line c) shows the results, where the maximum deviation is of about 0.7%. These results again suggests that the errors obtained in problem (b) were due to the numerical nonorthogonality at the control volume interfaces.

In |1| it is reported that errors in the solution of a similar problem were encountered due to the nonuniformity of the grid lines. The question which remains is wheter the errors are due to the existence of a nonzero β

(nonorthogonality) or due to the nonunformity of the grid with consequent error in the calculation of β at the interfaces.

Problem (d) - Nonorthogonal Grid - Uniformly Spaced

Fig.5(c) shows the grid employed. The GND and consequently the β values are nonzero. They are, however, because the grid is uniform, correctly calculated at the interfaces. Table 3 (line d) shows that the temperature field and hence the heat flux distribution is constant with ϕ.

These results demonstrate that in spite of having nonorthogonal grids the solution is the same as one obtained using orthogonal uniformly spaced grids. Again the results indicates that the errors in problem (b) are due to the wrong calculation of β at the interfaces. To clear this question the next test is presented.

Problem (e) - Nonorthogonal - Grid Nonuniformly Spaced

Table 3 (Line e) shows a non uniform heat flux distribution with ϕ . As already pointed out the reason is, probably, because the metric is not correctly calculated at the interfaces. To improve this value an average of the values at the center of the neighbouring cells is performed. The results obtained are presented in the same Table (line f) where it can be seen a considerable improvement, but the solution is still wrong. The same strategy, however, was used for the orthogonal nonuniform grid with complete success. To clarify this it is importante to have in mind that the GND must be the same for every ϕ for a constant radius (the grid is constructed in this way) for the grid shown in Fig.5(d). Averaging β from the values at the center of the cells will not guarantee (as it did for the problem (c)where GND is equal to zero) the same GND at the interfaces because now the GND is not zero, and so α and γ also take part in the calculations, according to Eq. (6).

6.CONCLUDING REMARKS

The solution of the laminar heat transfer problem in a quadricusped duct was obtained numerically using a quasi-orthogonal and a highly nonorthogonal discretization. Physical unrealistic results for the Nusselt number near the cusped corner were obtained with the highly nonorthogonal grid. In that region the Nusselt number, although very small, presented negative values. Perhaps with a finer grid the results could be improved.

These findings motivated the analysis of the effects of the grid nonorthogonality by solving a suitable heat conduction problem using different types of discretization. The main conclusion obtained with the solution of the heat

conduction problem is that β at the interfaces of the control volumes needs to be properly evaluated in order to represent the correct angle θ at the interface. However, when these cures were applied to the problem of the cusped region using a highly nonorthogonal grid the Nusselt number presented only a little improvement. There must be, then, other reasons for this behaviour. One possibility is the fact that, associated with the highly nonorthogonality of the grid, in the cusped region the velocity and the temperature are very small. The velocity times temperature appears in the source terms for the energy equation, making this term very small. A small error in the evaluation of the metrics and of the source term in this region may cause the Nusselt number to be negative. In fact,in the velocity problem where the source term is a constant, the friction coefficient (the equivalent of the Nusselt number in the thermal problem) shows erros of the order of only 1% of the maximum value.

In the other hand, the use of a quasi-orthogonal grid considerably improved the Nusselt number near the cusped corner. This permits to draw what is, perhaps, the most relevant conclusion of this work, concerning the generality of nonorthogonal codes. The quasi-orthogonal grid used was constructed without the need of obeying the orthogonality conditions and, because of that, it was very easy generated. It is also important to point out that the grid is quasi-orthogonal only near the corner, showing high GND in other regions. This flexibility permits to the numerical analyst to adjust the grid according to the physical phenomenon. Of course, it is always desirable to use coordinate systems as orthogonal as possible. The numerical model, by its turn, should be able to handle any type of discretization to claim for generality. The numerical example reported in this work clearly demonstrated this.

7.REFERENCES

1. J.C. Ferreri and M.A. Ventura,´On the Accuracy of Boundary Fitted Finite-Difference Calculations´,Int. J. for Num. Meth. in Fluids, 1984,4,359.
2. C.R. Maliska and G.D. Raithby,´A Method for Computing Three-Dimensional Flows Using Boundary-Fitted Coordinates´, Int. J. for Num. Meth. in Fluids, 1984,4,519.
3. C.W. Rapley,´Turbulent Flow in a Duct with Cusped Corners´, Int. J. for Num. Meth. in Fluids, 1985,5,155.
4. A.A. El-Hadik et al.,´A Study of Heat and Fluid Flow in Cusped Ducts in Laminar Case´, in Num. Meth. in Laminar and Turbulent Flow, C. Taylor, P.M. Gresho, M.D. Olson and W.G. Habashi, Eds., Pineridge Press, pp. 1069-1088, 1985.
5. J.F. Thompson et al.,´ Automatic Numerical Generation of Body-Fitted Coordinate Systems for Field Containing Any Number of Arbitrary TwoDimensional Bodies´, J. Comp. Phys.,1974,15,299.

SECTION 4

Application of Grid Generation to Technical Problems